Electronic Supplementary Material (ESI) for Physical Chemistry Chemical Physics.

# Supplementary Information: Controllable dissociation of $H_2O$ on $CeO_2$ (111) surface

J. Fan,[1] B. Xu,[2] J. Z. Zhao,[1] and H. Xu[1,a)]

[1]*Department of Physics, South University of Science and Technology of China, Shenzhen 518055, China*

[2]*Physics Department and Institute for Nanoscience and Engineering, University of Arkansas, Fayetteville, Arkansas 72701, USA*

---

a) Authors to whom correspondence should be addressed. Electronic addresses: xu.h@sustc.edu.cn

The calculations showed that our conclusions are independent on the surface termination or frozen layers. H atoms are used to saturate the dangling bonds of the $CeO_2$ (111) surface. Two different saturation models are considered: (1) only surface O atoms are saturated by H (denoted by Y1), and (2) both surface O and Ce are saturated by H (denoted by Y2). In addition, we checked the influences of the number of fixed layers on the strain induced dissociation of $H_2O$ on the stoichiometric $CeO_2$ (111) surface. The energy differences between the dissociative and molecular $H_2O$ on the stoichiometric $CeO_2$ (111) with the lattice strains of 0.00%, 1.29% and 2.40% are listed in Table S1. One can see that the energy difference and strain threshold are only quantitatively affected by surface termination or the number of frozen layers at the bulk-like side of the slab. Therefore, the calculated adsorption energies and the strain thresholds for water dissociation are not sensitive to slab models used in the calculations, and the conclusions regarding the strain-induced water dissociation is robust.

Table S1 Energy differences for the dissociative and molecular $H_2O$ on $CeO_2$ (111) surfaces with 0.00%, 1.29% and 2.40% tension strains. The models with different fixed layers and with/without –H at the bulk-like side of the slab were used.

| Total tri-layers | Fixed tri-layers | Without H (N)<br>H on O (Y1)<br>H on both O and Ce (Y2) | $\Delta E=E_{dis}-E_{mol}$ (eV) | | | Strain threshold (%) |
|---|---|---|---|---|---|---|
| | | | 0.00 % strain | 1.29 % strain | 2.40 % strain | |
| 5 | 0 | N | 0.06 | -0.05 | -0.13 | 0.73 |
| 7 | 0 | N | 0.05 | -0.05 | -0.13 | 0.65 |
| 7 | 1 | N | 0.05 | -0.05 | -0.12 | 0.67 |
| 7 | 2 | N | 0.06 | -0.05 | -0.13 | 0.73 |
| 7 | 3 | N | 0.06 | -0.05 | -0.12 | 0.74 |
| 7 | 4 | N | 0.06 | -0.05 | -0.13 | 0.73 |
| 5 | 0 | Y1 | 0.06 | -0.06 | -0.15 | 0.66 |
| 5 | 0 | Y2 | 0.05 | -0.06 | -0.12 | 0.62 |

Table S2 Bulk lattices of metal substrates, LEED patterns of the $CeO_2$ (111) surface with respect to the substrate and the lattice strain of the $CeO_2$ (111) surface deposited on different metal substrates.

| Substrate | Lattice (Å) | LEED pattern | Lattice strain |
|---|---|---|---|
| Pd (111) | 3.89 | $p(1.39\times1.39)$ | -0.05% |
| Pt (111) | 3.92 | $p(1.37\times1.37)$ | -0.73% |
| Rh (111) | 3.80 | $p(1.40\times1.40)$ | -1.66% |
| Ru (0001) | 2.70 | $p(1.40\times1.40)$ | -1.19% |

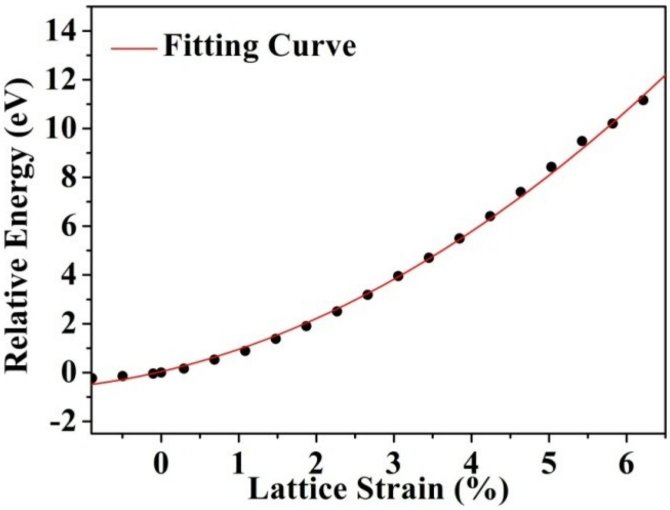

Fig. S1 The relative energy of the stoichiometric $CeO_2$ (111) surface as a function of the percentage of lattice strain. The energy of the $CeO_2$ (111) surface without the lattice strain is set to 0.

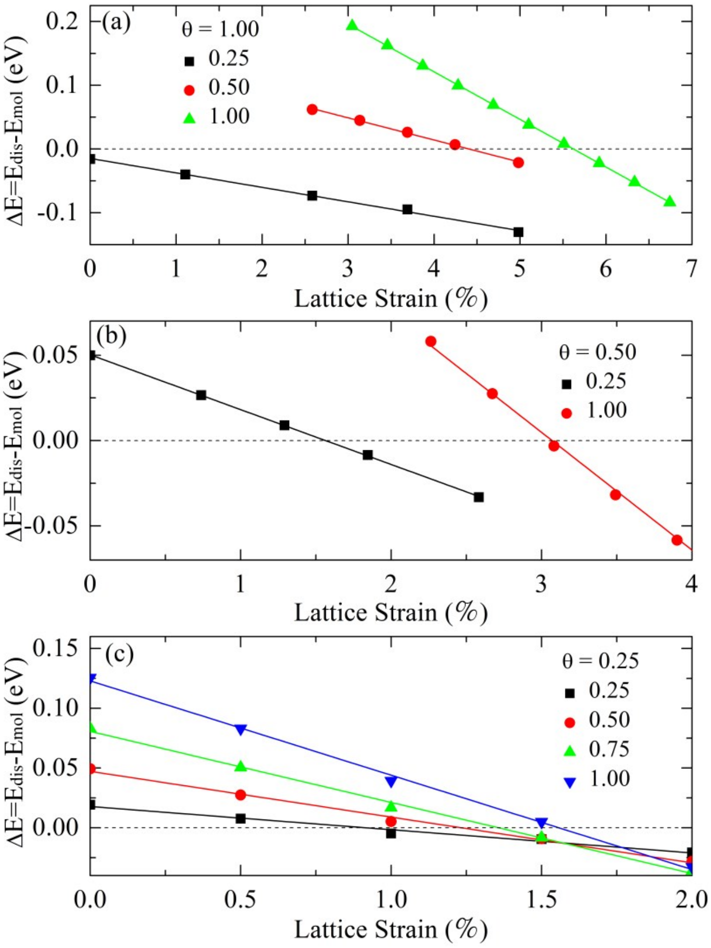

Fig. S2 Energy differences between each dissociative and molecular $H_2O$ on the stoichiometric $CeO_2$ (111) surface as a function of lattice strain at the $H_2O$ coverage of (a) 1.00, (b) 0.50 and (c) 0.25. For each coverages of $H_2O$, different dissociative ratios (e.g. the ratios of 0.25, 0.50, 0.75 and 1.00 for $\theta = 0.25$ in (c)) are calculated. The $p(2\times2)$ unit cell are used in (a) and (b), and $p(4\times4)$ unit cell are used in (c).

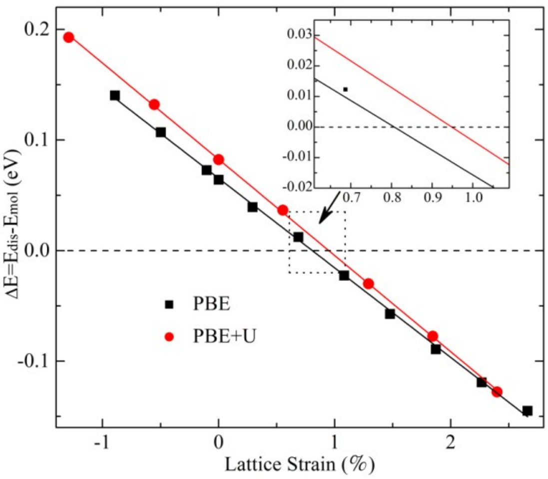

Fig. S3 The PBE and PBE+U results of energy differences between the dissociative and molecular $H_2O$ on the $p(3\times3)$ stoichiometric $CeO_2$ (111) surface as a function of lattice strain.

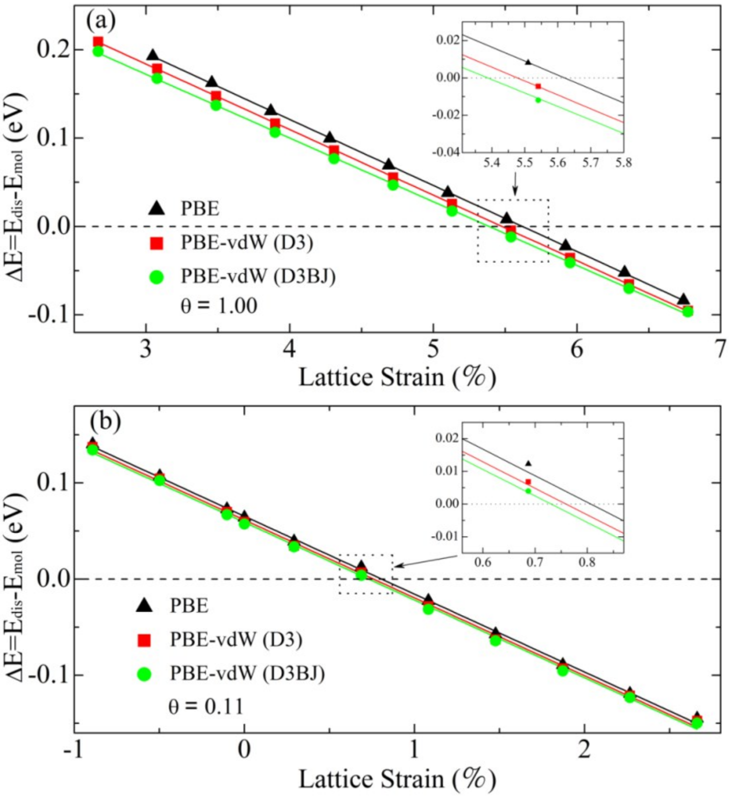

Fig. S4 The PBE and PBE-*vdW* results of energy differences between the dissociative and molecular $H_2O$ on the (a) $p(1\times1)$ and (b) $p(3\times3)$ stoichiometric $CeO_2$ (111) surface as a function of lattice strain.

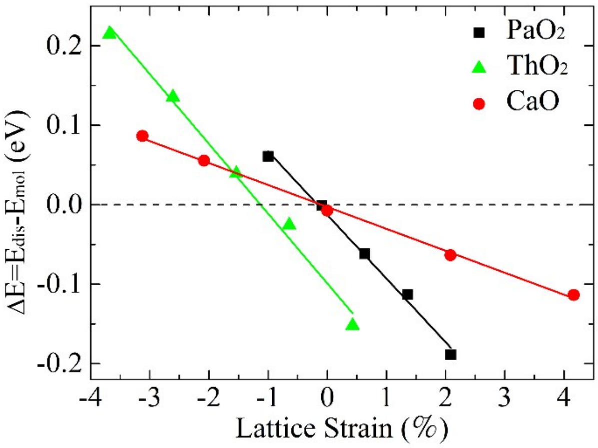

Fig. S5 PBE results of energy differences between the dissociative and molecular $H_2O$ on *p*(2×2) (111) surfaces of $PaO_2$ and $ThO_2$ with fluorite structure and the *p*(1×1) CaO (100) surface.

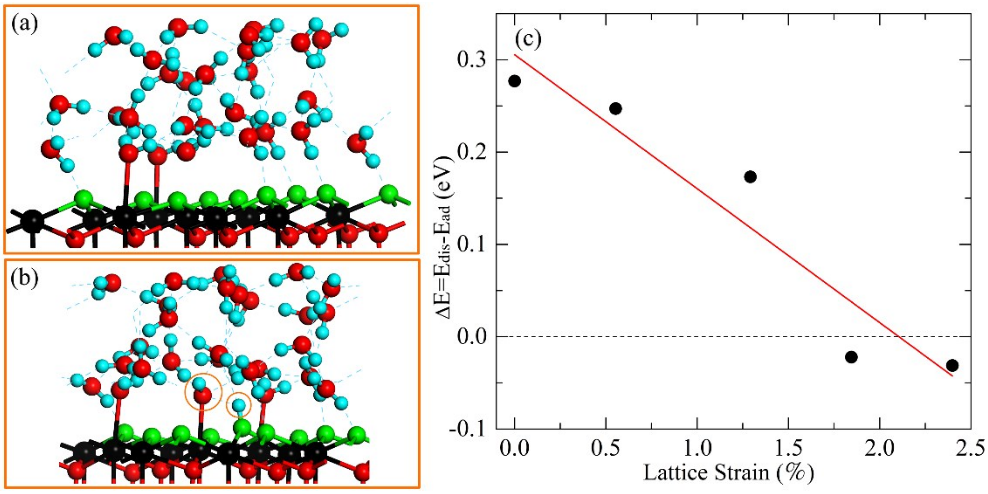

Fig. S6 (a) Side view of 3 ML $H_2O$ (27 $H_2O$ molecules) on the *p*(3×3) $CeO_2$ (111) surface. (b) One $H_2O$ molecule dissociates on the 3 ML $H_2O$-covered *p*(3×3) $CeO_2$ (111) surface. (c) The energy differences between the molecular adsorption structure in (a) and the dissociated one in (b) as a function of lattice strain.

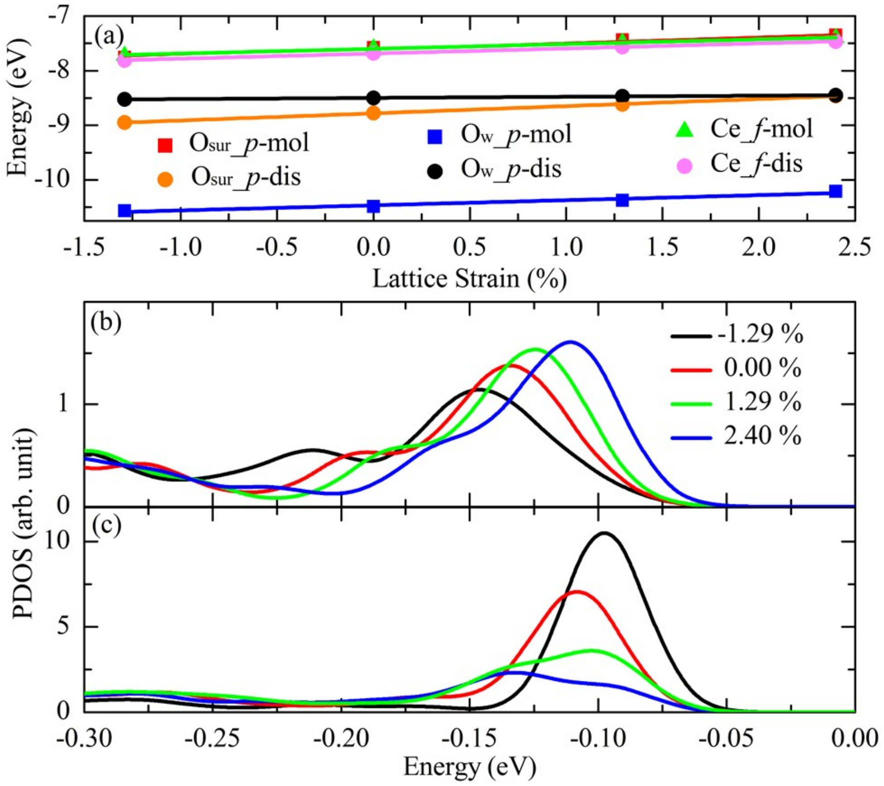

Fig. S7 (a) The band center positions as a function of lattice strain. The vacuum level is set to zero. The red squares, orange rounds, blue squares and black rounds represent the calculated band center of surface O-2*p* ($O_{sur}$_*p*-mol and $O_{sur}$_*p*-dis) and the adsorbed $H_2O$ ($O_w$_*p*-mol and $O_w$_*p*-dis), respectively. The green triangles and magenta rounds represent the calculated band center of surface Ce-4*f* (Ce_*f*-mol and Ce_*f*-dis), respectively. The corresponding linear fitting curves are presented. Here, the "-mol" and "-dis" mean the molecular and dissociative states of $H_2O$ on the surface. (b) The PDOS of surface Ce-4*f* on the stoichiometric $CeO_2$ (111) surface, and the Fermi level is set to zero. (c) The PDOS of O-2$p_y$ from the dissociated $H_2O$ on a *p*(3×3) $CeO_2$ (111) surface with the dissociative $H_2O$. The Fermi level is set to zero. The black, red, green and blue lines represent the corresponding PDOS under the strains of -1.29 %, 0.00 %, 1.29 %, and 2.40 %, respectively.

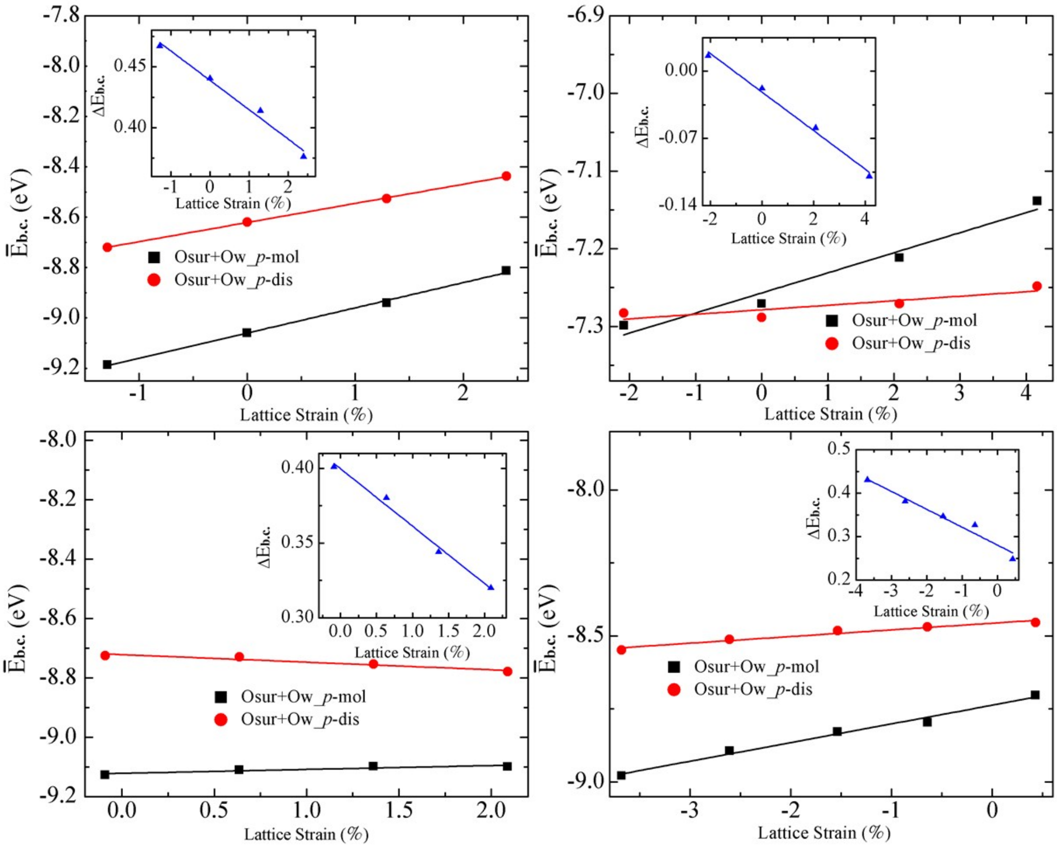

Fig. S8 The average *p* band center of $O_{sur}$ and $O_w$ for molecular and dissociative $H_2O$ on the stoichiometric (a) $CeO_2$ (111), (b) CaO (001), (c) $PaO_2$ (111), and (d) $ThO_2$ (111) surfaces. The average *p* band center is studied by calculating the whole *p* band. The insets show the difference of average *p* band center of $O_{sur}$ and $O_w$ for molecular and dissociative $H_2O$ as a function of lattice strain. $\Delta E_{b.c}$ denotes the energy difference of average *p* band center shift of both $O_{sur}$ and $O_w$ for dissociative and molecular $H_2O$.

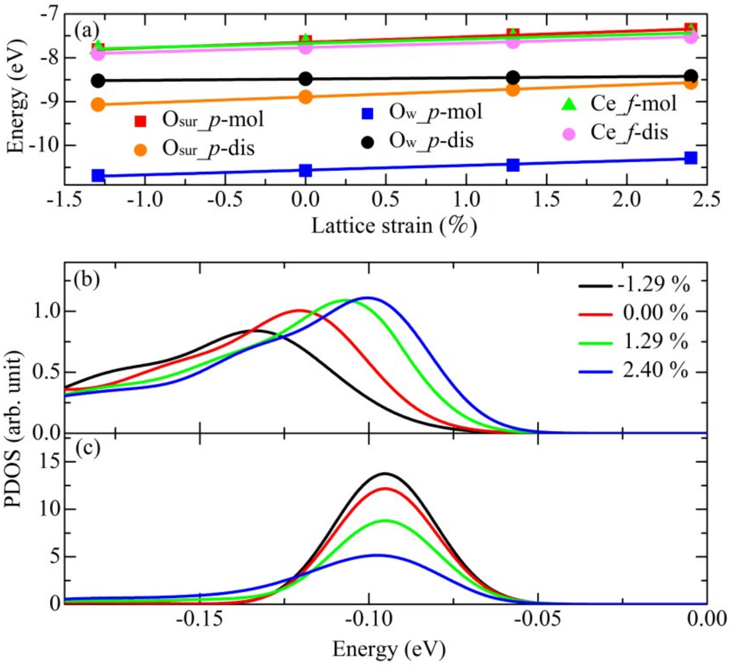

Fig. S9 (a) The PBE+U results of band center positions as a function of lattice strain. The vacuum level is set to zero. The red squares, orange rounds, blue squares and black round dots represent the calculated values of band center of surface O-2*p* ($O_{sur}$_*p*-mol and $O_{sur}$_*p*-dis) and the adsorbed $H_2O$ ($O_w$_*p*-mol and $O_w$_*p*-dis), respectively. The green triangles and magenta round dots represent the calculated values of band center of surface Ce-4*f* (Ce_*f*-mol and Ce_*f*-dis). The corresponding linear fitting curves are presented. Here, the "-mol" and "-dis" mean the molecular and dissociative states of $H_2O$ on the surface. (b) The PBE+U results of PDOS of surface Ce-4*f* on the stoichiometric $CeO_2$ (111) surface, and the Fermi level is set to zero. (c) The PBE+U results of PDOS of O-2$p_y$ from the dissociated $H_2O$ on a *p*(3×3) $CeO_2$ (111) surface with the dissociative $H_2O$. The Fermi level is set to zero. The black, red, green and blue lines represent the corresponding PDOS under the strains of -1.29 %, 0.00 %, 1.29 %, and 2.40 %, respectively.

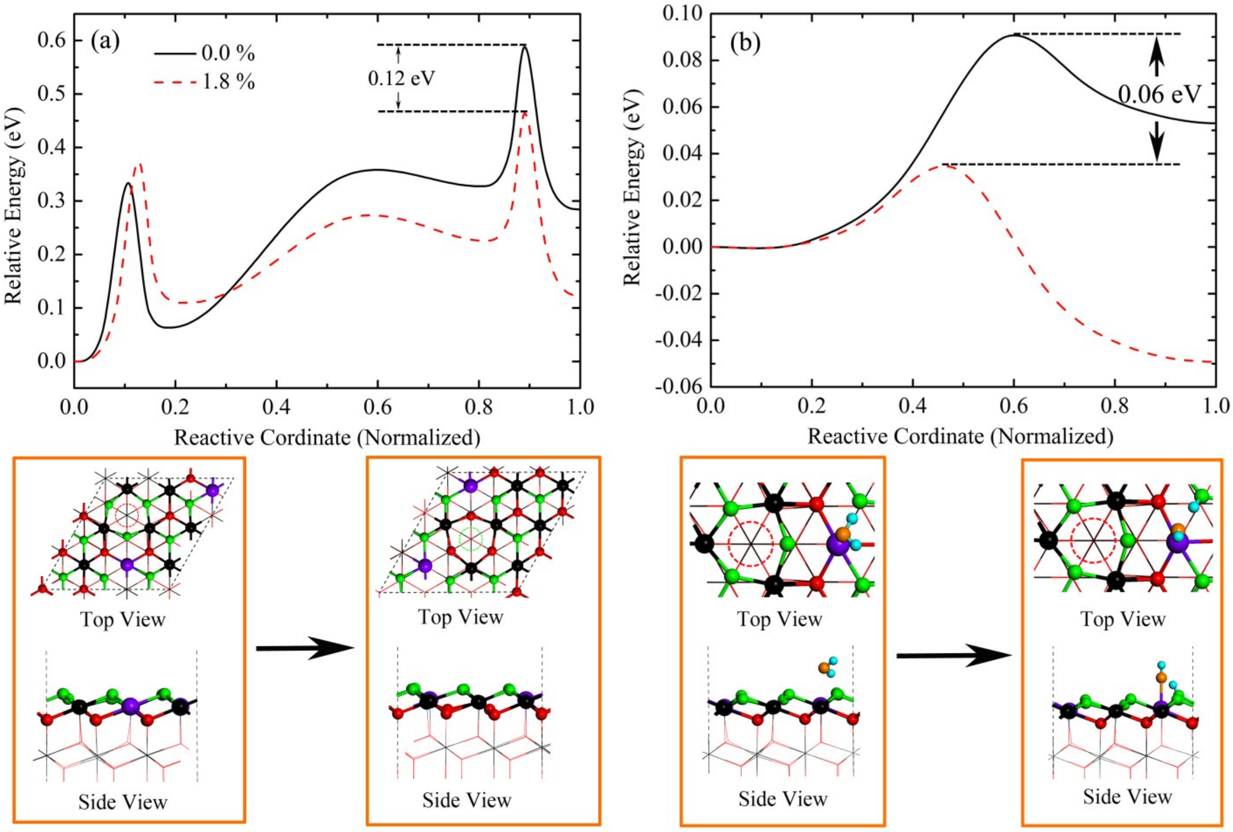

Fig. S10 (a) Potential energy profile for the migration of oxygen vacancy from the subsurface site to surface site under 0.0% and 1.8% tension strains on the $CeO_2$ (111) surface. (b) Potential energy profile for water dissociation on the $CeO_2$ (111) surface with a subsurface oxygen vacancy under 0.0% and 1.8% tension strains. The green and red dashed circles represent the surface and subsurface oxygen vacancies, respectively.